Title

High throughput quantification of battery solid electrolyte interphase conductivities and their use as solid state electrolytes

Author

Chen, Po-Hung

Publication Date

2023

Peer reviewed|Thesis/dissertation

UNIVERSITY OF CALIFORNIA

Los Angeles

High throughput quantification of battery solid electrolyte interphase conductivities and their use as solid state electrolytes

A thesis submitted in partial satisfaction

of the requirements for the degree Master of Science

in Chemical Engineering

by

Po-Hung Chen

2023

ABSTRACT OF THE THESIS

High throughput quantification of battery solid electrolyte interphase conductivities and their use as solid state electrolytes

by

Po-Hung Chen

Master of Science in Chemical Engineering

University of California, Los Angeles, 2023

Professor Yuzhang Li, Chair

As a key passivation layer that governs battery operation, the solid electrolyte interphase (SEI) has long been credited for enabling high performing batteries or blamed for their eventual death. However, qualitative descriptions of the SEI often found in the literature (e.g., “conductive”, “passivating”) highlight our incomplete understanding, where even the most basic properties foundational to SEI function (e.g., ionic and electronic conductivity) remain difficult to determine. Here, we propose a methodology to quantify SEI conductivities using a separator-free Cu|SEI|Li architecture that treats the SEI as a solid-state electrolyte. Although the non-ideal experimental setup leads to inconsistent and widespread SEI conductivity measurement, several improvement and failure analysis are discussed in this work. Perhaps most striking, we find that

reversible Li metal deposition is possible in our separator-less Cu|SEI|Li cell with additional liquid electrolyte, demonstrating that the SEI might be able to function like a solid-state electrolyte. However, the excess liquid electrolyte in the Cu|SEI|Li cell makes the argument of using SEI as solid state electrolyte somewhat questionable since SEI solely function as a passivated film and the lithium ions only come from the additional liquid electrolyte. Indeed, using SEI as solid state electrolyte remain challenging, but several future improvements are also discussed in this work. Our work provides quantitative measurement for how "conductive" and "passivating" SEI films and further enrich our understanding of the SEI, not just as a passivation layer to enable battery operation, but as a functional structure that can potentially have important implications for solid-state batteries.

The thesis of Po-Hung Chen is approved.

Philippe Sautet

Carlos Gilberto Morales Guio

Yuzhang Li, Committee Chair

University of California, Los Angeles

2023

Table of Contents

1 Introduction **1**

2 SEI Conductivity Measurement **4**

2.1 Various iteration of Cu|SEI|Li architecture 5

2.2 AC impedance for ionic conductivity measurement 9

2.3 DC polarization for electronic conductivity measurement 18

3 SEI as solid state electrolyte **21**

3.1 Li deposition and reversible cycling in Cu|SEI|Li architecture 21

4 Future work **25**

5 Method **27**

6 Appendix **30**

7 Concluding Remarks **33**

8 References **34**

List of Figures

Figure 1. Schematic of various iteration Cu|SEI|Li cell (a) version 1 (b) version 2 (c) version 3. 8

Figure 2. Schematic of new (a) Li|SEI|Li and (b) Cu|SEI|Li cell 8

Figure 3. Schematic of the physical battery components for SEI ionic conductivity measurement 13

Figure 4. Equivalent circuit model for Cu|SEI|Li cell 13

Figure 5. Nyquist plot of the EIS data (green dots) and the fitting result (the red line) for Cu|SEI|Li cell 14

Figure 6. Schematic of the charge transfer process (arrows) at SEI and PE donut shaped separator 15

Figure 7. Schematic of the physical battery components for SEI electronic conductivity measurement 19

Figure 8. Schematic of the DC polarization curve for SEI electronic conductivity measurement 20

Figure 9. Voltage profile of lithium deposition at 0.01 mA cm^{-2} and 0.22 mAh cm^{-2} in Cu|SEI|Li cell with swollen state 4M LiFSI in DME SEI 23

Figure 10. Voltage profile of cycling at 0.01 mA cm^{-2} and 0.05 mAh cm^{-2} in Cu|SEI|Li cell with swollen state 4M LiFSI in DME SEI 23

Figure 11. SEM images of lithium deposition at 0.01 mA cm^{-2} and 0.22 mAh cm^{-2} in Cu|SEI|Li cell with swollen state 4M LiFSI in DME SEI 24

Figure 12. SEM images of SEI surface after one hour drying condition 24

Acknowledgements

This work comes from the contribution of numerous individuals. I would like to thank the external scientific collaborators, peers, and mentors who contributed to my projects in some ways (Qingyang Yin and Jinhui Xu from the Lu Lab) and my labmates from the Li Group (among many others Xintong Yuan, Bo Liu, and Katelyn Lyle). My deepest gratitude goes to my advisor Professor Yuzhang Li for this opportunity of growth and for his guidance throughout my Master's program.

I would also like to express gratitude to Professor Philippe Sautet and Professor Carlos Gilberto Morales Guio for being on my committee and reviewing this work.

1 Introduction

Since first proposed by Peled in 1979, the concept of a solid electrolyte interphase (SEI) surface film that allows ions to flow (while blocking electrons) has shaped our modern understanding of battery operation.[1–3] As a self-passivating film, the SEI enables highly reactive anode materials (e.g., Li metal, lithiated graphite, Si etc.) to operate beyond the voltage stability window of the liquid electrolyte, as its continuous electrochemical decomposition is inhibited by the electronically insulating SEI.[4–6] A large body of work introduces several strategies (e.g., electrolyte engineering, artificial coatings, host materials, etc.) to empirically modify the SEI for improved battery performance.[7–10] Liquid electrolyte engineering has emerged as a powerful approach to tune deposition morphology of the high-capacity Li metal anode by tailoring SEI chemistry and nanostructure. In particular, electrolytes that favor decomposition of anions and fluorinated components have been shown to form an SEI film that is "conductive" and "passivating" to facilitate reversible and uniform Li deposition.[11–15] These qualitative descriptions are attributed to the highly fluorinated and anion-derived chemistry of the SEI. More recently, cryogenic-electron microscopy (cryo-EM) experiments have shown electrolytes can infiltrate into the SEI to varying degrees, resulting in an important swelling phenomenon that also correlates strongly with the Coulombic efficiency (CE) of the Li electrodeposition process.[16,17] Unfortunately, we lack insight into how SEI chemistry or swelling states quantitatively impact SEI properties, representing a large gap in our understanding for battery design. Instead, we are currently limited to using SEI chemistry, nanostructure, or swelling state as qualitative proxies to indirectly rationalize observed improvements in battery performance.

While its basic function as an ionic conductor and electron insulator make SEI one of the most important aspects of a battery, SEI conductivities remain the least understood and

quantified within the existing literature.[18–21] Quantifying SEI ionic and electronic conductivities across various SEI chemistries and swelling states would be a significant breakthrough that bridges the knowledge gap of how electrolyte formulations directly impact SEI properties (and eventual battery performance). For example, we might expect advanced electrolytes to form SEI films with high ionic conductivity to facilitate uniform Li growth and low electronic conductivity for improved passivation and reduced electrolyte degradation; we would expect the opposite for poor performing electrolyte chemistries. However, direct measurement of SEI properties remains challenging and a technique to quantify SEI conductivities across various swelling states does not currently exist.

Here, we introduce a simple Cu|SEI|Li architecture that rapidly quantifies both ionic and electronic conductivity of SEI films formed under diverse conditions (e.g., electrolyte chemistry, swelling state). Whereas conventional wisdom would suggest that placing Cu into direct contact with Li metal induces a short circuit, we show that an open circuit voltage of ~1.6 - 2.4 V once the Li foil has been passivated by an SEI film. As an ionically conductive yet electronically insulating layer, the SEI in this unique architecture prevents shorting by functioning precisely as a solid state electrolyte (SSE), which is a clear departure from the traditional view of SEI as merely a surface corrosion film.[22,23] This unorthodox yet subtle shift in perspective opens a broad range of approaches within the solid state battery literature to make high-throughput SEI conductivity measurements possible.[24–26] Although our Cu|SEI|Li architecture is non ideal for a consistent and reliable conductivity measurement, several improvements and solutions (e.g., Li|SEI|Li architecture) are discussed in the following section for future research. Furthermore, we discover that reversible Li plating and stripping is possible in our separator-less Cu|SEI|Li architecture. However, the addition of liquid electrolyte in the Cu|SEI|Li architecture is needed

for reversible Li plating and stripping indicating that SEI might only act as a passivated film in this case and the lithium ions are coming solely from the liquid electrolyte rather than the lithium metal electrode. On the other hand, SEI film under dry condition will form cracks on the surface and eventually leading to shorting of Cu|SEI|Li cell. Indeed, the SEI as an SSE remain challenging due to above issues. Nevertheless, this paradigm shift towards recognizing the SEI as an SSE still opens up exciting possibilities to quantify other key SEI properties that are normally only associated with liquid and solid state electrolytes (e.g., transference numbers).[27–32]

2 SEI Conductivity Measurement

Previously, Rui et al.[18] proposed a methodology for single phase and native SEI ionic conductivity measurement, they report the preparation of single-component SEIs of lithium oxide (Li2O) grown ex situ on Li foils by controlled metal–gas reactions, generating "deconstructed" model interfaces with a nanoscale thickness (20–100 nm) similar to the native, yet more complex multiphasic SEI. The model Li|Li2O electrodes serve as a platform for further chemical and electrochemical characterization. In particular, electrochemical impedance spectroscopy (EIS), combined with interface modeling, is used to extract ionic conductivity of Li|Li2O in symmetric cells with EC/DEC electrolytes. However, their SEI conductivity measurement is limited to swollen state SEI measurement due to the liquid electrolyte presence in the system. The ionic conductivity of dry state SEI is unable to obtain with their experimental setup. Therefore, A novel setup enabling both swollen state and dry state SEI ionic conductivity measurement is needed.

For SEI electronic conductivity measurement in the literature, Caleb et al.[20] proposed a nanometer-resolution three-dimensional technique that enables ex-situ mapping of electronic resistivity of SEI formed on a model single-crystalline wafer Si anode. Their experimental approach uses scanning spreading-resistance microscopy resistance imaging. Park et al.[21] reported their experimental result on the measurement of the electrical resistivity of SEI (covers uniformly on the surface of the graphite anode) using the direct-contact technique based on electron microscopy combined with 4-point-probe micro-electrical method. However, a simple and high throughput SEI electronic conductivity measurement for SEI formed chemically on lithium metal anode does not currently exist.

The scope of this initial study will be to quantify the SEI electronic and ionic conductivity using our Cu|SEI|Li architecture. To prepare the Cu|SEI|Li cell, we first form SEI films by immersing pristine Li foil in the liquid electrolyte for 48 hours (see methods). After the SEI was formed, we then put the pre-made SEI into type 2032 coin cells by placing Cu into direct contact with the SEI-passivated Li metal without a separator. The SEI conductivity measurement is tested under two conditions: swollen state and dry state. The swollen state SEI is defined as pre-made SEI with additional 10 μL liquid electrolyte and the dry state SEI is defined as SEI under 30 minutes drying without any electrolyte added. The separator-less Cu|SEI|Li cell does not short circuit and exhibits an open circuit voltage of ~1.6 - 2.4 V. We then use AC impedance and DC polarization (common methods in the solid state electrolyte literature) to measure SEI ionic and electrical conductivity.[33–38] This chapter will mainly focus on the finding of the above experimental setup, methodology, failure analysis for current setup and future improvement.

2.1 Various iteration of Cu|SEI|Li architecture

In this chapter, a Cu|SEI|Li architecture is proposed for rapid SEI conductivity measurement (AC impedance for ionic conductivity measurement and DC polarization for electronic conductivity measurement). Various iteration of Cu|SEI|Li architecture will be presented, and oversights in the current setup are identified and analyzed. Based on our previous finding, we proposed the final experimental setup which are Li|SEI|Li cell for ionic conductivity and Cu|SEI|Li for electronic conductivity measurement with external pressure.

Version 1: As shown in Fig. 1(a), our first version of Cu|SEI|Li architecture is direct contact of SEI passivated lithium metal and Cu foil with two Cu wires attach to BioLogic battery tester. There are several drawbacks in this experimental setup. For example, the point contact between Cu wires and lithium, Cu electrode is highly non-uniform creating inconsistent interfacial resistance and thus making the conductivity measurement inaccurate. Furthermore, shorting happens since the SEI formation process is cast drop 60 μL onto the lithium metal for 48 hours and the outer rim of lithium metal (20 mm in diameter) is not fully passivated with SEI. Therefore, when we directly place Cu foil (12 mm in diameter) onto the SEI passivated lithium, Cu can contact the bare lithium metal on the outer rim so that the Cu|SEI|Li architecture will short. To address these issues, we need to integrate the version 1 Cu|SEI|Li architecture into a coin cell architecture to enable uniform contact. Besides, we need to put a PE (polyethylene) donut shaped separator to make sure only the center part of SEI passivated lithium contacts the Cu foil so that shorting will not happen with our setup.

Version 2: As shown in Fig. 1(b), we integrate the Cu|SEI|Li architecture into a coin cell geometry. However, one downside of this version 2 setup is that the PE donut shaped separator is placed between SEI and Cu creating some space between SEI and Cu (not direct contact).

Version 3: As shown in Fig. 1(c), we put the PE donut shaped separator in between positive case and Cu foil to make sure there is direct contact between Cu and SEI passivated lithium. However, the Cu size is too big (12 mm in diameter) so that it will contact the outer rim of SEI passivated lithium and shorting of the setup will happen (similar to the issue in version 1). To address this issue but also make sure there is direct contact between SEI and Cu, we decrease the size of Cu from 12 mm in diameter to 6.35 mm (quarter inch) in diameter. In this iteration, we can address the shorting issue and enable uniform contact between interfaces.

Final version (for future research): The current version 3 setup still have some issues such as using asymmetric rather than symmetric setup for ionic conductivity measurement, wrong donut shaped separator material selection (the separator should be ionic and electronic insulated) and external pressure should be applied to the coin cell to minimize interfacial resistance. (Further detailed analyze will be presented in the following section.) In conclusion, we propose a new version of Li|SEI|Li architecture for SEI conductivity measurement and Cu|SEI|Li architecture in Fig. 2 for SEI conductivity measurement for a reliable and consistent measurement.

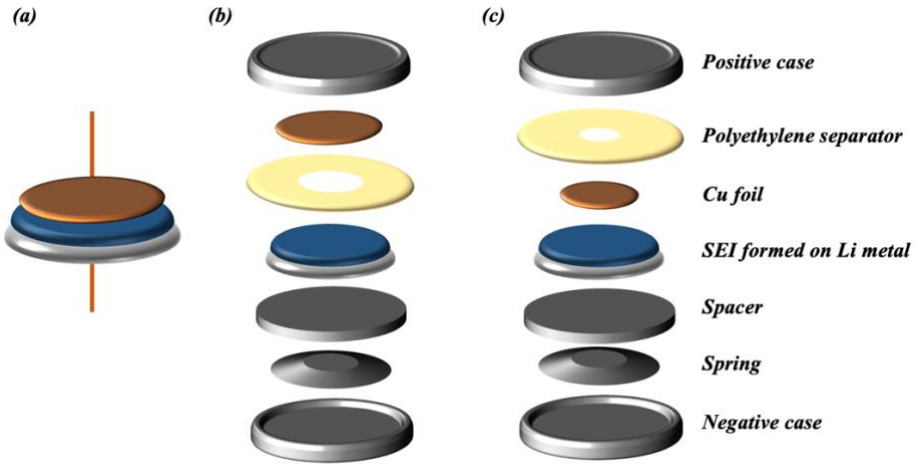

Figure 1. Schematic of various iteration Cu|SEI|Li cell

(a) version 1 (b) version 2 (c) version 3

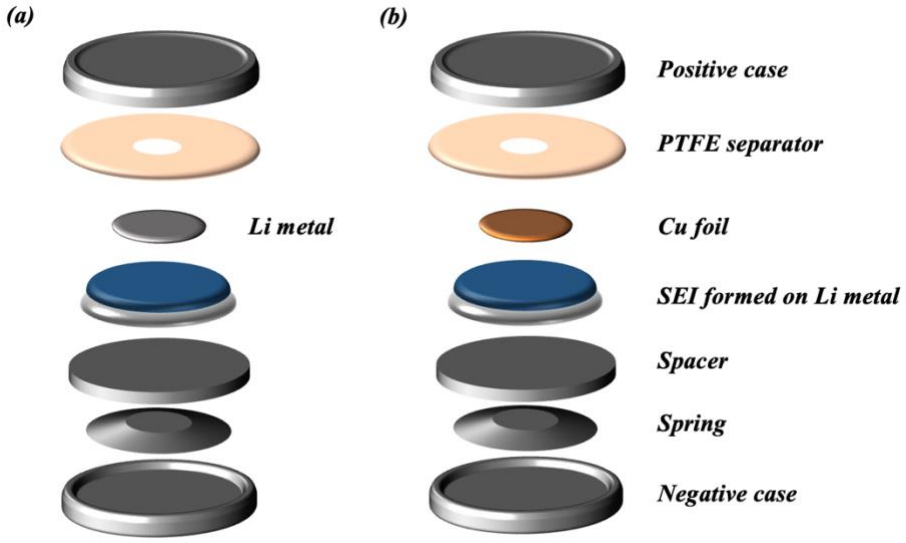

Figure 2. Schematic of new (a) Li|SEI|Li and (b) Cu|SEI|Li cell

2.2 AC impedance for ionic conductivity measurement

Electrochemical impedance spectroscopy (EIS)[39–45] is a technique used to characterize the electrical behavior of electrochemical systems. It provides information about the electrochemical processes occurring at the interface between electrodes. EIS works by applying a small amplitude alternating voltage signal to the electrochemical system over a wide range of frequencies. The resulting current response is measured, and the impedance of the system is determined. Impedance is the ratio of the applied voltage to the measured current response and is a complex quantity consisting of a real component and an imaginary component. The AC signal used in EIS typically varies from very low frequencies (millihertz) to high frequencies (megahertz). EIS can capture a detailed impedance spectrum that provides information about various electrochemical processes and properties of the system by sweeping through a specific frequency range. The impedance spectrum is often presented in a Nyquist plot, where the imaginary component of impedance is plotted against the real component. The Nyquist plot typically consists of a semicircular portion at high frequencies and a linear portion at low frequencies. When the AC voltage is applied, the electrochemical system undergoes cyclic changes in potential. This alternating potential with varying frequencies drives various electrochemical reactions, including charge transfer processes at the electrode-electrolyte interface and ion transport within the electrolyte. For example, we can use a parallel RC circuit (R: resistance, C: capacitance) as an equivalent model to represent the charge transfer process at the electrode surface where the transfer of charge happens in parallel with the charging of the double layer capacitance. To further understand why there is a semi-circle in the Nyquist plot, we need to introduce mathematical model to the analysis. In parallel, the admittances (i.e., the

reciprocals of the impedances) are additive: $\frac{1}{Z} = \frac{1}{R} + jwC$ (where Z is the total impedance, R is the resistance, w is the frequency and C is the capacitance). If we rearrange that equation for Z (by first multiplying all the terms by R) then we end up with: $Z = R/(1 + jwRC)$. From this equation you can see that at high frequency, i.e., *w* is very close to infinity, the lower term on the fraction goes to infinity, so the impedance tends towards zero; the ideal circuit behaves like the capacitor at infinite frequency – it has zero impedance. At low frequency, i.e., *w* is very close to zero, the bottom term becomes one, so the total impedance of the circuit equals R meaning that with a direct current, the circuit behaves like a resistor. Because when *w* is very close to zero (basically a direct current), the capacitor becomes fully charged and the current only goes through the resistor. By analyzing the mathematical model, we can derive the Nyquist plot for this circuit which is a semicircle, intercepting the real axis at 0 and R. Therefore, by analyzing the impedance spectra, various electrochemical parameters can be extracted, such as the solution resistance, charge transfer resistance, double-layer capacitance, ionic conductivity, and diffusion coefficients. These parameters can help understand the kinetics of electrochemical reactions, the performance of electrochemical devices, and the properties of electrolyte materials.

In this study, we aim to investigate the ionic resistance of SEI by the Cu|SEI|Li cell (solid-electrolyte interphase passivating films formed on lithium combined with a copper blocking electrode), To describe the charge transfer process within the SEI, we adopted a relatively simple equivalent circuit model based on empirical analysis. Churikov et al. compared various equivalent circuit options and developed an equivalent circuit model that considers the physical behavior and meaning of each component.[46,47] The physical meaning of the proposed equivalent circuit model will be illustrated in the following section:

1. Space-Charge Region at the SEI-Li Interface, C_{SC} (capacitor)[26,46,47]:

Due to the differences in chemical potential between lithium and the passivated SEI layer, the mutual diffusion of ionic and electronic charge carriers is required to align interfacial energy levels. Therefore, a space-charge region is formed at their interface. A space charge region refers to a region near the interface where there is an imbalance or accumulation of charge carriers. It typically occurs at the boundary between the electrode and the electrolyte or between different layers or materials within the electrode. The formation of a space charge region is often influenced by the presence of different concentrations of ions or the movement of charged species across the interface. For example, when an electrode is immersed in an electrolyte or two different layers of material, positive and negative ions from the electrolyte can migrate to the electrode surface, creating a charge imbalance. This results in the formation of a space charge region where the concentration of ions or charge carriers is different from that of the bulk electrolyte. This space-charge layer is modeled as a capacitance, C_{SC}.

2. Accumulation/Depletion of Charge Carriers at the SEI-Cu Interface, C_{SEI} (capacitor)[26]:

When an interface is presence between two materials (SEI/Cu), a layer of charged species is formed at the interface due to the differences in chemical potential. The interface consists of a layer of adsorbed ions of opposite charge to the electrode surface and a region of diffuse ions in the SEI. During EIS measurements, the applied AC voltage induces the charging and discharging of the interface which behaves like a capacitor. As a result, charge carriers can be accumulated or depleted at the interface. The accumulation or depletion of ionic and electronic charge carriers across the boundary of the SEI layer and the Cu blocking electrode is

modeled as a geometric capacitance at the SEI/Cu interface, C_{SEI}.

3. Ionic Resistance of the SEI Layer, R_{SEI} (resistance):

The ionic resistance within the SEI layer is modeled as a resistance, R_{SEI}.

4. Solid-State Diffusion at the Space-Charge Region, W (Warburg impedance)[48]:

The Warburg impedance is observed as a diagonal line with a slope of 45 degrees in the Nyquist plot of EIS data. It is represented by a straight line that extends towards the lower frequencies without intersecting the real axis. This characteristic behavior is indicative of a diffusion-limited process. In the context of solid-state diffusion, the Warburg impedance arises from the movement of charge carriers through a solid material, such as an electrode or an electrolyte. It reflects the impedance resulting from the diffusion process, where charge carriers diffuse into and out of the material over time. The solid-state diffusion of ionic and electronic charge carriers within the space-charge region is modeled as a Warburg element, W.

5. Residual Liquid Electrolyte Resistance:

To account for the ionic resistance of the residual liquid electrolyte in swollen-state EIS measurements, a resistance component, Re, is included in the model. A hypothesis here is that the resistance component, Re should be able to account for the liquid influence in our ionic conductivity measurement.

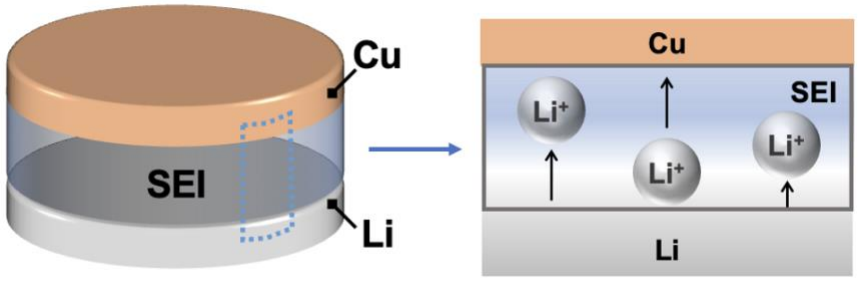

Figure 3. Schematic of the physical battery components for SEI ionic conductivity measurement

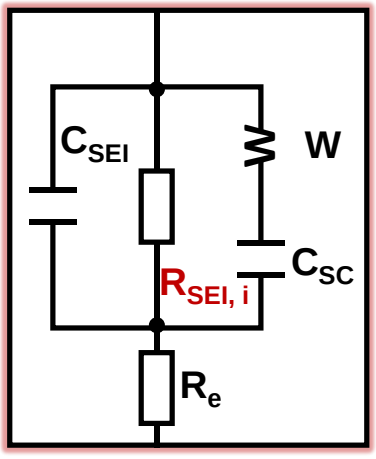

Figure 4. Equivalent circuit model for Cu|SEI|Li cell

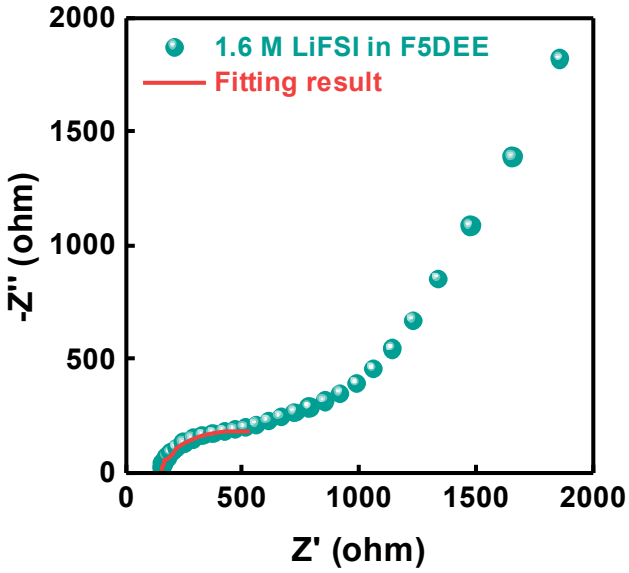

Figure 5. Nyquist plot of the EIS data (green dots) and the fitting result (the red line) for Cu|SEI|Li cell

By applying the proposed equivalent circuit model to our experimental setup, we should be able to extract the SEI ionic resistance information from the fitting result. The model provides good fit to some of our swollen state EIS measurements. However, some finding from this experiment setup and methodology shows that the current Cu|SEI|Li cell experimental setup and the methodology that we apply are not valid mainly because of the following reasons.

1. The donut shaped polyethylene separator that was used in our Cu|SEI|Li cell experimental setup is ionically conductive. Here we performed a simple experiment to verify this finding. A Cu|PE|Li coin cell with 1M LiPF6 in EC/DEC liquid electrolyte is built. Here we replace the normal separator with the PE separator that was used in our conductivity measurement. The goal of this experiment is whether the PE separator can function as a traditional separator that is normally used in a coin cell. Therefore, we perform lithium deposition with the Cu|PE|Li coin cell and find out that we can see lithium deposited onto the

Cu foil showing that the PE membrane is ionically conductive. As shown in Fig. 6, the finding invalids our previous ionic conductivity measurement since one hypothesis that is applied is that the charge transfer process only happens within the SEI layer and the interface which are attach to the SEI layer. However, if the PE separator is ionically conductive, the charge transfer process could be happening at both the SEI layer and the PE separator as shown in Fig. 6 making the analysis of the Nyquist plot and model fitting not valid. To fix the issue, we will need to find an alternative donut shape membrane material which is both electronic and ionic passivated to validate the ionic conductivity measurement.

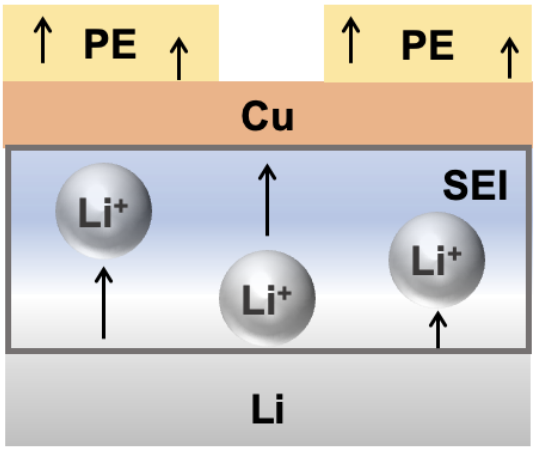

Figure 6. Schematic of the charge transfer process (arrows) at SEI and PE donut shaped separator

2. The definition of swollen state SEI which is adding 10 μL to the pre-made SEI is non-ideal. A hypothesis of swollen state SEI ionic conductivity measurement is that the addition of liquid electrolyte will not affect the R_{SEI} value that we extract from the equivalent circuit model since the liquid electrolyte resistance term, Re should be able to account for the liquid electrolyte

influence of our swollen state setup. However, the R_{SEI} value that we measure increase about one to two orders of magnitude showing that the influence of additional liquid electrolyte should not be neglected, and it further complicates the analysis of our ionic conductivity measurement. One possible solution is to redefine the definition of swollen state SEI. There should be no liquid electrolyte added so that we further remove the excess liquid on the pre-made SEI layer.

3. The contact of our Cu|SEI|Li is not ideal. In both the swollen state and dry state SEI ionic conductivity measurement, we find that a consistent and reliable Nyquist plot with a distinct semi-circle is hard to obtain. Since a donut shaped separator is used in our Cu|SEI|Li setup, the contact between the Cu foil and the positive case through the centered hole of the donut shaped separator is non-uniform and creating non-consistent interfacial impedance. This is the main reason why we are unable to get reliable Nyquist plot with EIS. Applying moderate pressure with a battery crimper would be a potential solution, since improving contact between interfaces is often observed with higher pressure in traditional solid state electrolyte literature.[49–51] However, the remaining challenge is that applying high pressure such as 1000 psi could result in breakage of SEI and leading to shorting issue. The optimal pressure to apply for ionic conductivity measurement still requires further experiment to obtain.

4. The asymmetric Cu|SEI|Li cell experimental setup is not suitable for ionic conductivity measurement of SEI. In solid state electrolyte literature, a symmetric cell experimental setup is used for ionic conductivity measurement of solid state electrolyte because of the following advantage.[26]

a. Simplicity: The symmetric setup simplifies the experimental configuration by eliminating the need for complex electrode designs or asymmetric geometries. It involves using identical electrodes on both sides of the solid-state electrolyte, making the measurement setup easier to assemble and replicate.

b. Avoiding polarization effect[26,52]: In asymmetric setups, where different materials or geometries are used for the electrodes, polarization effects can occur due to uneven charge distribution or concentration gradients. These polarization effects can interfere with the accurate measurement of ionic conductivity. By using a symmetric setup, the electrode polarization is minimized, leading to more reliable conductivity measurements.

c. Reducing contact resistance[26,52]: The symmetric setup helps to minimize the contact resistance between the electrodes and the solid-state electrolyte. When different materials or interfaces are involved, the contact resistance can vary and affect the overall measurement. Using identical electrodes in a symmetric setup ensures consistent contact properties, allowing for more accurate determination of ionic conductivity.

By adopting the above failure analysis to our current Cu|SEI|Li setup, we proposed a new setup that could potentially address the above issued, enabling accurate and reliable SEI ionic conductivity measurement. The new setup is symmetric SEI conductivity measurement where two SEI passivated lithium are form and combine as a Li|SEI|Li architecture. We can minimize the contact resistance and avoid polarization effect that was dominant in our previous asymmetric Cu|SEI|Li setup. Furthermore, to minimize the influence from the additional liquid electrolyte (resulting in lower R_{SEI} value obtained from the equivalent circuit of EIS data fitting), we remove any excess liquid electrolyte on the SEI layer with Kimwipes for swollen state SEI conductivity measurement. We also replace our initial polyethylene donut shaped separator with PTFE donut shaped separator (which is not ionic and electronic conductive) to ensure the charge transfer process when conducting EIS measurement is solely happening at the SEI layer and its interfaces. In the end, after we assemble the Li|SEI|Li cell, some pressure (from 500 psi to 1000 psi) is applied to the Li|SEI|Li cell to further decrease the interfacial

contact resistance and

improve the contact in our experimental setup. The new Li|SEI|Li cell will be used in our future SEI ionic conductivity measurement.

2.3 DC polarization for electronic conductivity measurement

The Hebb-Wagner method is a technique used to measure the electronic conductivity in materials with mixed ionic and electronic conductivity.[53–56] In our Cu|SEI|Li experimental setup, we employ the Hebb-Wagner method to measure the electronic conductivity of the solid-electrolyte interphase (SEI) formed directly on lithium metal, using a reversible lithium metal electrode and a Cu foil blocking electrode. The SEI acts as a mixed ionic and electronic conductor, where both ions and electrons migrate within the cell. The reason why we use an asymmetric cell setup instead of a symmetric cell setup for DC polarization is because we need the concentration gradient of ionic charge carriers to build up at Li/SEI interface so that it can counteract the polarization (1V) applied. Therefore, we can immobilize the ionic charge carriers and only measure the current from electrons. With a Li symmetric cell setup, the concentration gradient is hard to maintain at a certain interface. By employing the Hebb-Wagner method, we aim to exclude the ionic current originating from ion migration and focus solely on measuring the electronic current.

In our Cu|SEI|Li architecture, we apply a constant DC polarization of 1V. Initially, all charge carriers, including Li ions, migrate towards the lithium metal electrode. However, since the Cu foil, serving as the blocking electrode, does not provide ion sources, a concentration gradient of lithium ions is established at the interface between the lithium metal and the SEI. Over time, at steady state, the diffusion of lithium ions towards the Cu electrode counteracts the

applied polarization, resulting in no net lithium-ion flux within the SEI. At steady state, the measured current is solely attributed to electronic carriers as shown in Fig. 8. By measuring this steady-state current, we can determine the electronic conductivity of the SEI. The exclusion of ionic current allows us to focus specifically on the electronic current and accurately measure the electronic conductivity of the SEI. Once the steady-state electronic current is obtained from the DC polarization, we can use the formula: electronic conductivity (σe) = L / (R × A)

where L is the thickness of the SEI, A is the area of the Cu ion blocking electrode, and R is the

SEI electronic resistance obtained from Ohm's law, V = I × R where V is the applied constant voltage, and I is the measured steady-state current.

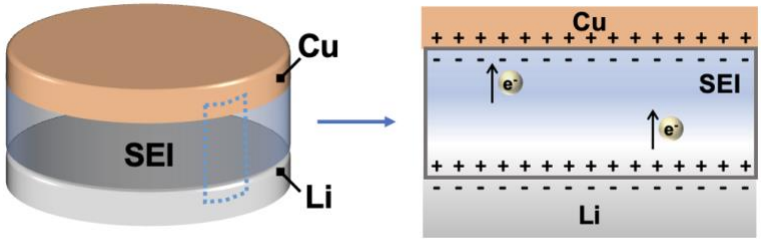

Figure 7. Schematic of the physical battery components for SEI electronic conductivity measurement

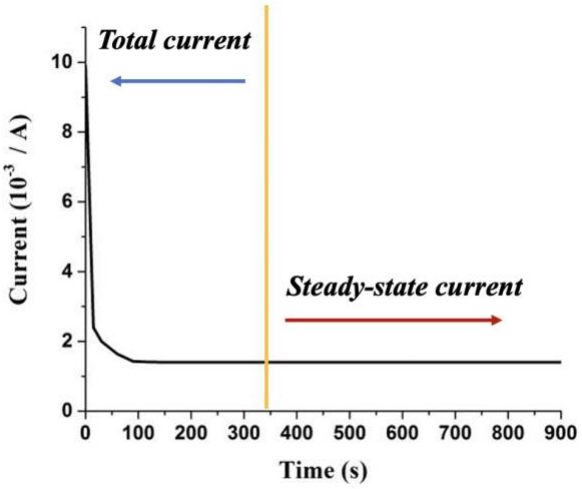

Figure 8. Schematic of the DC polarization curve for SEI electronic conductivity measurement

However, wide variations of steady state current (almost one order of magnitude) are observed with the methodology. There are two potential reasons for this inconsistent SEI electronic conductivity measurement. As previously mentioned in SEI ionic conductivity measurement, the PE donut shaped separator is ionic conductive and for the swollen and dry state SEI, we add additional liquid electrolyte in the experimental setup. This non-ideal setup and experimental condition will lead to unclear polarization data interpretation since whether the measured steady state current is from polarization of SEI layer or PE donut shaped separator is hard to decouple.

One potential solution for a more accurate SEI electronic conductivity is by replacing the PE separator (which is ionically conductive), to the PTFE membrane (which is not ionically conductive). Besides, the swollen and dry state SEI measurement should not have any excess liquid electrolyte in the system to make sure that the steady state current obtain from the DC

polarization method is only coming from the ion migration and polarization of SEI layer. By adopting the above strategies, a more consistent and accurate SEI electronic conductivity measurement could be conducted for future research.

3 SEI as solid state electrolyte

Although our above methodology and analysis on SEI conductivity is not fully developed yet, our Cu|SEI|Li cell setup showing no shorting with direct contact of Cu and SEI passivated lithium shows that SEI does function as an electron passivated layer and is ionically conductive based on the above EIS analysis. In principle, the SEI should then be able to function as a solid state electrolyte, enabling the reversible plating and stripping of metallic Li.

3.1 Li deposition and reversible cycling in Cu|SEI|Li architecture

To demonstrate this proof-of-concept in our separator-less Cu|SEI|Li cell geometry, we perform standard galvanostatic cycling at 0.01 mA/cm2 for a deposition capacity of 0.05 mAh/cm2 and a stripping cutoff voltage of 1 V vs. Li metal. The voltage profile of this electrodeposition process on the Cu current collector using our SEI as an SSE is displayed in Fig. 9 and 10 (SEI is in its swollen state, formed in 4M LiFSI in DME). We detect the familiar nucleation overpotential of Li onto Cu and the voltage plateaus of Li plating and stripping, which are the precise features observed in voltage profiles of traditional Cu-Li half cell geometries. Scanning electron microscopy (SEM) confirm that Li metal is deposited in our Cu|SEI|Li cell and appears to be non-dendritic, which is a favorable morphology as shown in Fig. 11. Remarkably, this reversible Li deposition and stripping occurs at room temperature across a thin SEI (~3 um) as the SSE without excess applied pressure. However, both of our

lithium deposition and Cu|SEI|Li cell are conducted in swollen state condition meaning that 10 μL of additional liquid electrolyte is added into the system. In this case, the SEI may just be functioning as a separator to prevent shorting from direct contact of lithium and Cu electrode. The lithium deposition and cycling voltage profile come from the lithium ion in the additional liquid electrolyte rather than from the lithium negative electrode, and the ion conductive donut shaped PE separator also might serve as a separator for lithium deposition and cycling. To further address the issue and enabling SEI to function as a solid state electrolyte, we remove any excess liquid electrolyte by rinsing the SEI with solvent and dry the SEI in the glovebox for one hour. Surprisingly, when the SEI without any liquid electrolyte is integrate into our Cu|SEI|Li cell, shorting of the Cu|SEI|Li cell is observed. To further analyze why shorting is happening within the Cu|SEI|Li cell, top view SEM images of SEI without any excess liquid is observed in Fig. 12. The SEI layer is no longer uniformed under one hour drying condition and cracks in the SEI layer can be observed leading to shorting of our Cu|SEI|Li cell. This finding can be explained by the SEI swelling behavior since the thickness/volume of SEI can vary between swollen state and dry state.[16] The swelling behavior can lead to contraction of SEI during the drying process and cracks of SEI can form leading to exposed lithium metal underneath. The finding shows that further SEI engineering is needed for a SEI with minimum swelling behavior to show this proof-of-concept using SEI as solid state electrolyte.

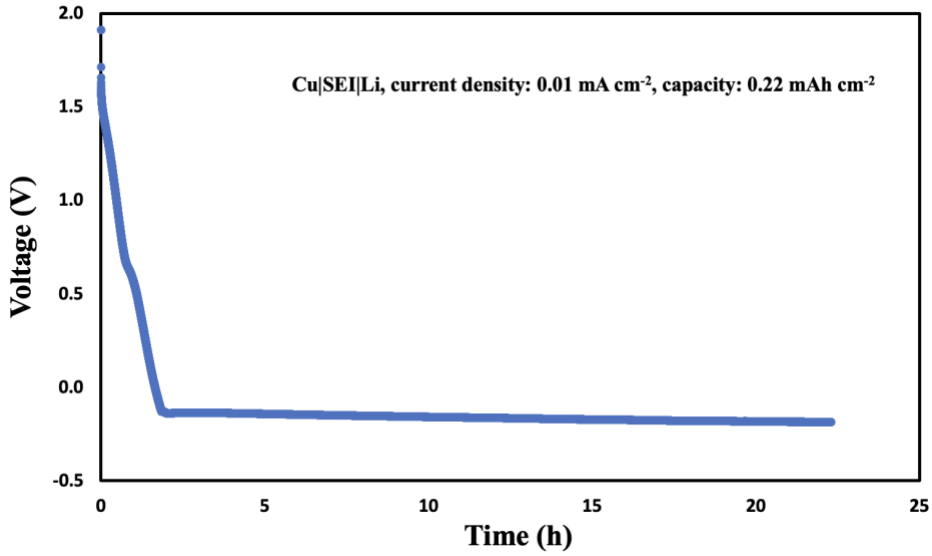

Figure 9. Voltage profile of lithium deposition at 0.01 mA cm^{-2} and 0.22 mAh cm^{-2} in Cu|SEI|Li cell with swollen state 4M LiFSI in DME SEI

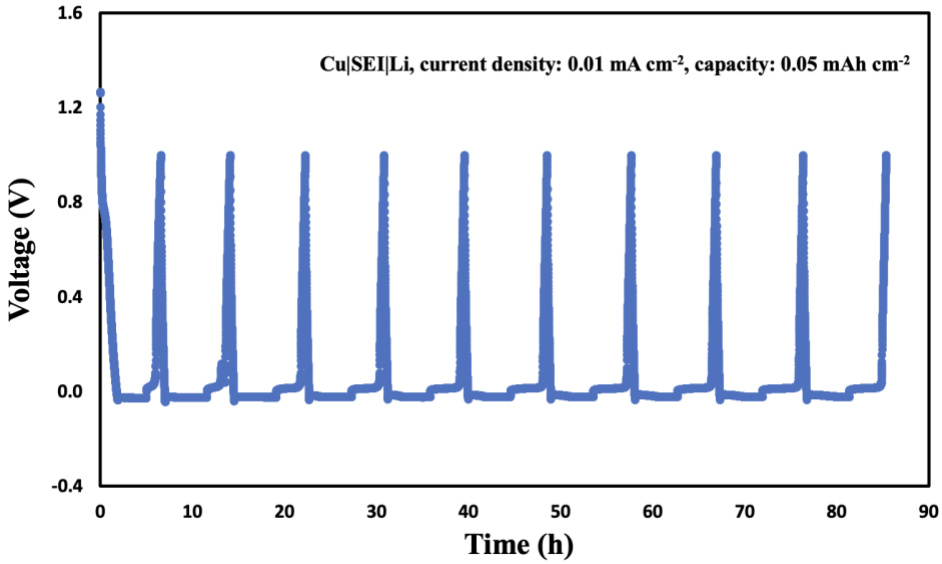

Figure 10. Voltage profile of cycling at 0.01 mA cm^{-2} and 0.05 mAh cm^{-2}

in Cu|SEI|Li cell with swollen state 4M LiFSI in DME SEI

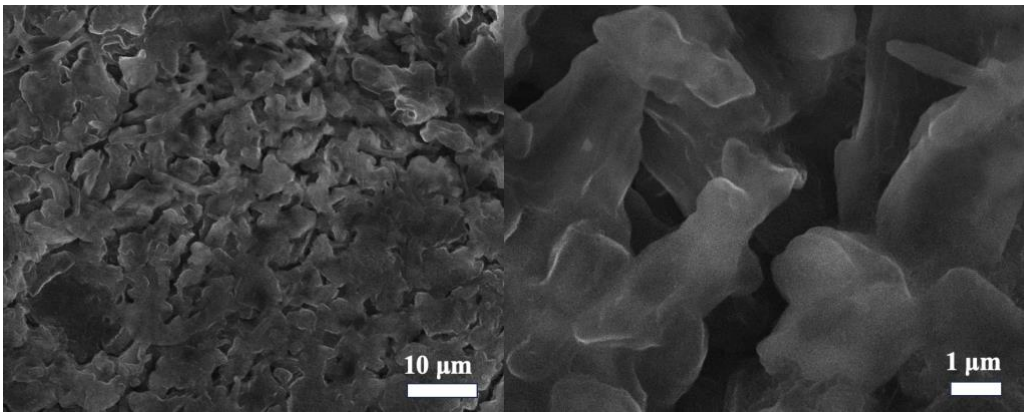

Figure 11. SEM images of lithium deposition at 0.01 mA cm^{-2} and 0.22 mAh cm^{-2} in Cu|SEI|Li cell with swollen state 4M LiFSI in DME SEI

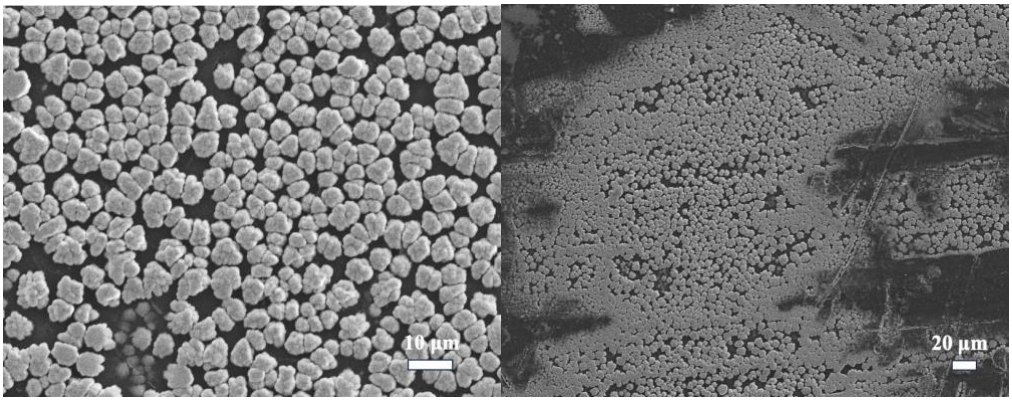

Figure 12. SEM images of SEI surface after one hour drying condition

4 Future work

Combining the above failure analysis, a new Li|SEI|Li cell architecture is proposed for a more consistent and reliable SEI ionic conductivity measurement. With the new Li|SEI|Li, we can characterize the SEI ionic conductivity in different electrolyte systems and swelling states. The SEI swelling ratio is quantified by cryo-EM imaging of electrolyte infiltration into the SEI and calculated by dividing the thickness of SEI in the swollen state by that of SEI in the dry state. SEI swelling ratios can range from 1.2 (low swelling) to 2.3 (high swelling) in various electrolytes and correlates with Coulombic efficiency.[16] One hypothesis is that the absence or presence of a liquid in the SEI film will dramatically impact how Li ions travel through the SEI layer. This future research can potentially bring new insight in explaining the dewetting and dry process during battery cycling. The diverse swelling states and ionic conductivity of SEI could induce the formation of a notched structure, which would eventually pinch off to create electrically isolated Li from the current collector.[57] The dewetting process during battery cycling will facilitate dead Li formation and accelerate capacity loss.[58,59] The future research will revise our previous understanding of Li ion transport through the SEI and has important implications for the impact of dewetting processes on cycling stability.

For SEI electronic conductivity measurement, an ionically and electronically passivating PTFE donut shaped separator is integrated into our current Cu|SEI|Li cell, enabling a more precise polarization of SEI layer. Therefore, accurate and reliable steady state current and SEI electronic conductivity can be obtained. In the literature, liquid electrolyte engineering has emerged as a powerful approach to tune deposition morphology of the high-capacity Li metal anode by tailoring SEI chemistry and nanostructure. Electrolytes that favor

decomposition of anions and fluorinated components have been shown to form an SEI film which has higher Coulombic efficiency (CE). However, how does anions and fluorinated components in SEI boost the battery performance remain unclear and not much quantitative analysis has been shown in literature.[60–62] With our new SEI electronic conductivity measurement, we can study the correlation between SEI films that formed under various electrolytes chemistry and their electronic conductivity. One hypothesis we proposed is that the SEI films with higher ratio of anions and fluorinated components have lower electronic conductivity (more passivated to electrons transfer between liquid electrolyte and lithium metal electrode) leading to lower capacity loss during battery cycling.

More remarkably, in this initial study, we proposed a Cu|SEI|Li architecture to demonstrate SEI can potentially function as a solid state electrolyte. Although the addition of liquid electrolyte in the system and the SEI crack formation after drying process make using SEI as solid state electrolyte remain challenging. Indeed, more Cu|SEI|Li architecture setup engineering is needed. For example, thinner donut shaped separator with applied pressure to the Cu|SEI|Li cell can improve the contact between interfaces in the cell and thus minimize the interfacial impedance of the system. Furthermore, to address the SEI cracks formation in dry condition, SEI formed under different electrolyte systems should be further investigate. The goal is to find a certain SEI which has minimum swelling behavior under drying condition to mitigate the cracks of SEI films and prevent the lithium metal from contacting the Cu electrode leading to shoring of the SEI cell.

5 Method

Assembly and construction of Cu|SEI|Li geometry:

Our unique Cu|SEI|Li geometry is constructed in two steps: (1) SEI formation on metallic Li foil and (2) standard coin cell assembly by direct contact between SEI-passivated Li metal and Cu foil. These steps are described below.

SEI formation on metallic Li foil:

1. In an Ar-filled glove box, Scrape surface of metallic Li foil using a clean razor blade to expose pristine Li surface.
2. Assemble a simple version of the coin cell by stacking the negative case, the spacer, and 20 mm diameter lithium metal. Pipette 60 microliters of liquid electrolyte into the cell. Cover the system with the positive case to prevent liquid electrolyte evaporation.
3. Rest the coin cell in the glove box at room temperature for 48 hours. The SEI will form chemically in this period.
4. Disassemble the coin cell to extract the SEI-passivated Li metal foil.
5. To form a swollen SEI in the present study, add 10 microliters of liquid electrolyte to the SEI-passivated lithium and immediately proceed to the Cu|SEI|Li cell assembly procedure.

To form a dry SEI in the present study, let the SEI-passivated lithium rest in the glove box for 30 minutes so that liquid electrolyte within the SEI may evaporate before moving onto the following procedure.

Cu|SEI|Li Cell Assembly:

1. This system resembles a standard coin cell system with the omission of the traditional separator. Stack the negative case (at the bottom), spring, and spacer with the SEI-passivated lithium in the glove box.

2. Place a Cu foil with 0.31 cm^2 area on top of the SEI-passivated lithium.

3. Place a donut shaped polyethylene separator on top of the Cu foil. (This is to prevent shorting from contact of positive case and other cell components.)

4. For SEI conductivity measurement, place a positive case on top without crimping the cell. For SEI as solid state electrolyte use, crimp the cell under 1000 psi to improve contact.

Li|SEI|Li Cell assembly:

1. This system resembles a standard coin cell system with the omission of the traditional separator. Stack the negative case (at the bottom), spring, and spacer with the SEI-passivated lithium in the glove box.

2. Stack positive case (at the bottom), PTFT donut shaped separator and a pristine Li foil with 0.2 cm^2 area and apply pressure with a spacer on top of the Li foil manually (improve the contact between battery components).

3. Assemble the components obtain in setup 1 and 2 by placing the positive case on top (along with the battery components in step 2) of the SEI passivated lithium (along with the

battery components in step 1).

4. Use the battery crimper to apply 1000 psi pressure to the Li|SEI|Li cell (improve contact of solid-solid interfaces).

SEI as solid state electrolyte coin cell testing.

Assembled coin cells with SEI as solid state electrolyte were loaded onto a battery cycler (BioLogic) and deposited lithium onto the Cu substrate under 0.01 mA/ cm^2 current density until shorting happened. The SEI as solid state electrolyte coin cells cycled under 0.01 mA/ cm^2 current density for 5 hours (capacity: 0.05 mAh/ cm^2) and the cut-off voltage for stripping is 1V.

Cross-section SEM sample preparation.

Place the SEI-passivated lithium into the coin cell and attach it to the battery clamp of BioLogic for 5 minutes. This step is to make sure the SEI thickness we measure are identical to the real measurement condition. After clamping the SEI-passivated lithium, rinse the SEM sample with solvent (DEC or DME) to remove excess salt on the sample surface. Cut a small opening on the SEI-passivated lithium disk with scissors, and then slowly tear the sample apart with two tweezers. The cross-section of SEI will expose and ready for SEM thickness characterization.

6 Appendix

SEI thickness characterization

To further calculate the SEI ionic and electronic conductivity, cross-section scanning electron microscopy (SEM) images were taken for 5 electrolyte chemistry SEI. Thickness in the following figures were determined from measurement at more than 30 random positions on the edges of the cross-section views. For each SEI electrolyte chemistry, we present an example of SEI cross-section image and a SEI thickness histogram.

(a) 1 M $LiPF_6$ in EC/DEC

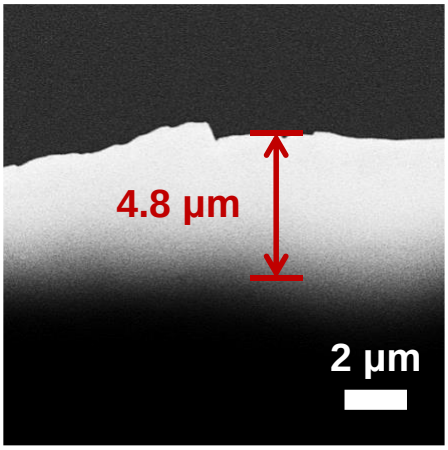

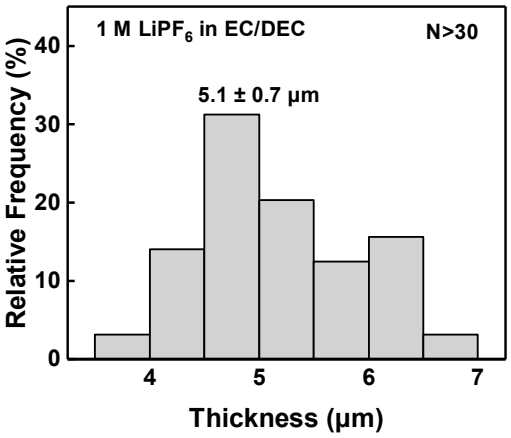

(b) 1 M $LiPF_6$ in EC/DEC/FEC

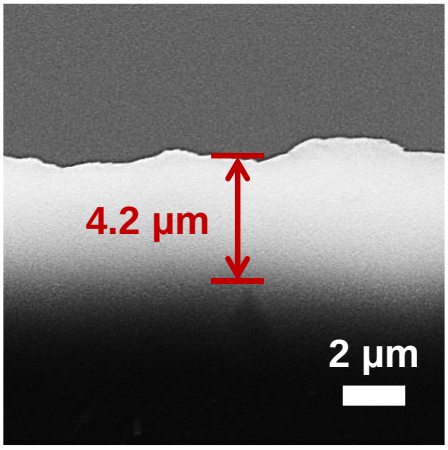

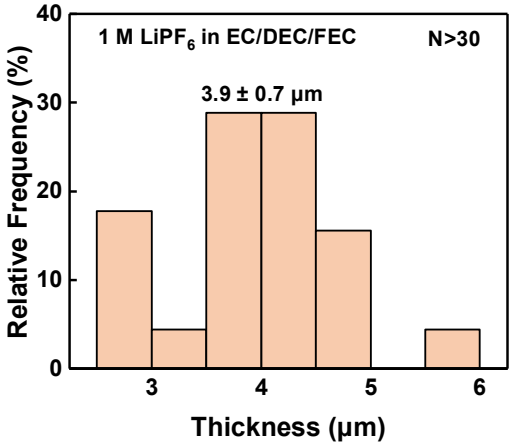

(c) 1 M LiFSI in DME

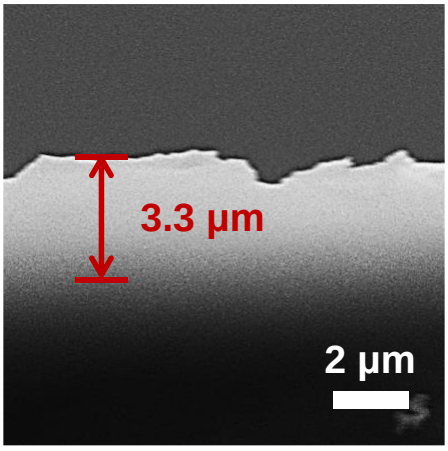

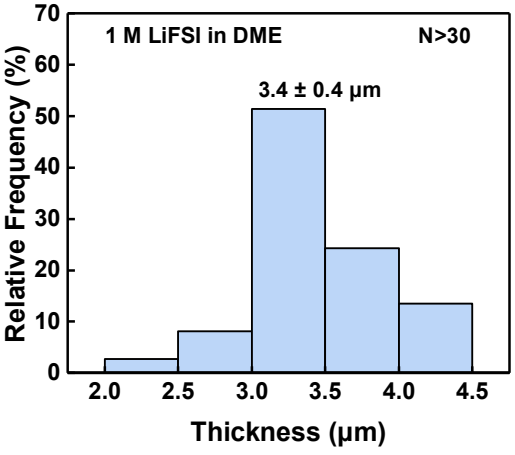

(d) 4 M LiFSI in DME

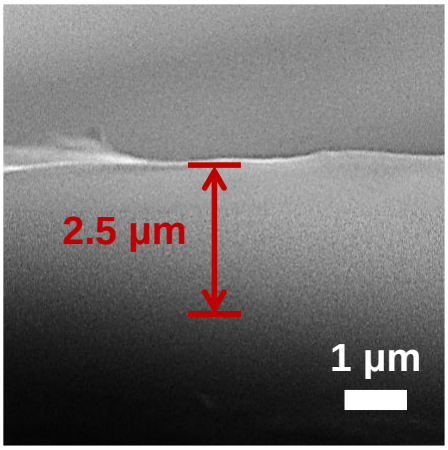

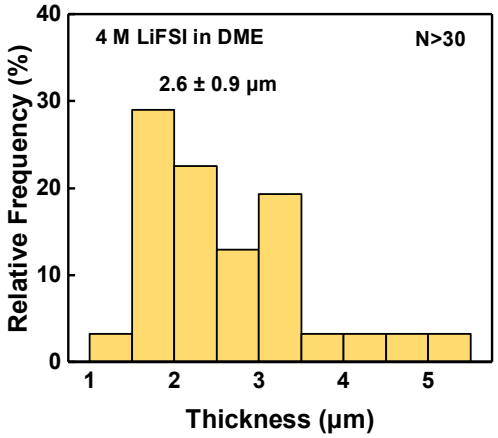

(e) 1.6 M LiFSI in F5DEE

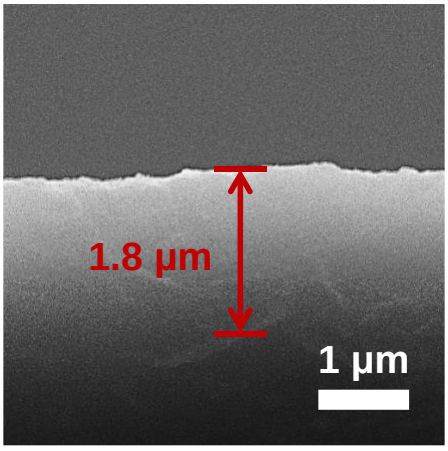

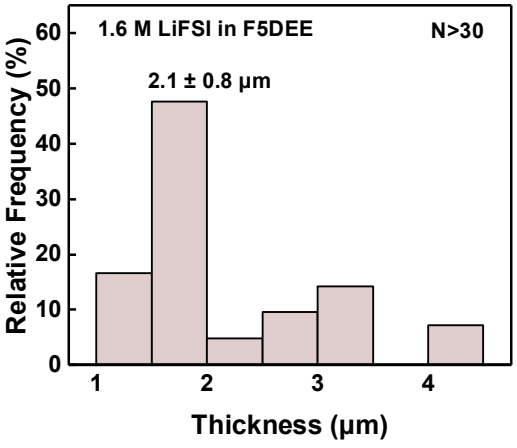

7 Concluding Remarks

In conclusion, the goal is to develop a simple and high throughput platform that will transform how we discuss the SEI, transitioning from historically qualitative descriptions towards new quantitative measurements. Although, the Cu|SEI|Li cell experimental setup is non-ideal for SEI conductivity measurement and the definition of swollen state SEI (addition of liquid electrolyte into the system) is not suitable for SEI conductivity measurement causing further complication when analyzing the data, several failure analysis and future improvement are proposed in the thesis including our new Li|SEI|Li cell setup and replacement of PE separator to PTFE separator which is both ions and electrons passivated. Furthermore, an idea that challenge the existing paradigm for what an SEI layer can be is proposed which is using SEI to function as solid state electrolyte. Indeed, the cell architecture and the optimal electrolyte chemistry to engineer an ideal SEI for the application are remain unclear, but future research can potentially open up exciting possibilities to make a solid state battery with SEI as solid state electrolyte.

8 References

1. Peled, E. The Electrochemical Behavior of Alkali and Alkaline Earth Metals in Nonaqueous Battery Systems—The Solid Electrolyte Interphase Model. *J. Electrochem. Soc.* **126**, 2047 (1979).
2. Aurbach, D. Review of selected electrode–solution interactions which determine the performance of Li and Li ion batteries. *Journal of Power Sources* **89**, 206–218 (2000).
3. Peled, E., Golodnitsky, D. & Ardel, G. Advanced model for solid electrolyte interphase [SEI] electrodes in liquid and polymer electrolytes. *Journal of the Electrochemical Society* **144**, (1997).
4. He, D., Lu, J., He, G. & Chen, H. Recent Advances in Solid-Electrolyte Interphase for Li Metal Anode. *Front Chem* **10**, 916132 (2022).
5. Xu, K. Nonaqueous Liquid Electrolytes for Lithium-Based Rechargeable Batteries. *Chem. Rev.* **104**, 4303–4418 (2004).
6. Verma, P., Maire, P. & Novák, P. A review of the features and analyses of the solid electrolyte interphase in Li-ion batteries. *Electrochimica Acta* **55**, 6332–6341 (2010).
7. Yan, K. *et al.* Selective deposition and stable encapsulation of lithium through heterogeneous seeded growth. *Nature Energy* **1**, 16010 (2016).
8. Cheng, X.-B., Zhang, R., Zhao, C.-Z. & Zhang, Q. Toward Safe Lithium Metal Anode in Rechargeable Batteries: A Review. *Chem. Rev.* **117**, 10403–10473 (2017).
9. Liu, W. *et al.* Artificial Solid Electrolyte Interphase Layer for Lithium Metal Anode in High-Energy Lithium Secondary Pouch Cells. *ACS Appl. Energy Mater.* **1**, 1674–1679 (2018).

10. Tu, Z. *et al.* Designing Artificial Solid-Electrolyte Interphases for Single-Ion and High-Efficiency Transport in Batteries. *Joule* **1**, (2017).

11. Yu, Z. *et al.* Rational solvent molecule tuning for high-performance lithium metal battery electrolytes. *Nat Energy* **7**, 94–106 (2022).

12. Zhang, E., Chen, Y., Yu, Z., Cui, Y. & Bao, Z. Monofluorinated Ether Electrolyte with Acetal Backbone for High-Performance Lithium Metal Batteries. Preprint at https://doi.org/10.48550/arXiv.2305.19580 (2023).

13. Fluorinated solid electrolyte interphase enables highly reversible solid-state Li metal battery | Science Advances. https://www.science.org/doi/10.1126/sciadv.aau9245.

14. He, M., Guo, R., Hobold, G. M., Gao, H. & Gallant, B. M. The intrinsic behavior of lithium fluoride in solid electrolyte interphases on lithium. *Proceedings of the National Academy of Sciences* **117**, 73–79 (2020).

15. Tan, J., Matz, J., Dong, P., Shen, J. & Ye, M. A Growing Appreciation for the Role of LiF in the Solid Electrolyte Interphase. *Advanced Energy Materials* **11**, 2100046 (2021).

16. Zhang, Z. *et al.* Capturing the swelling of solid-electrolyte interphase in lithium metal batteries. *Science* **375**, 66–70 (2022).

17. Li, Y. *et al.* Atomic structure of sensitive battery materials and interfaces revealed by cryo–electron microscopy. *Science* **358**, 506–510 (2017).

18. Guo, R. & Gallant, B. M. Li2O Solid Electrolyte Interphase: Probing Transport Properties at the Chemical Potential of Lithium. *Chem. Mater.* **32**, 5525–5533 (2020).

19. Guo, R., Wang, D., Zuin, L. & Gallant, B. M. Reactivity and Evolution of Ionic Phases in the

Lithium Solid–Electrolyte Interphase. *ACS Energy Lett.* **6**, 877–885 (2021).

20. Stetson, C. *et al.* Three-dimensional electronic resistivity mapping of solid electrolyte interphase on Si anode materials. *Nano Energy* **55**, 477–485 (2019).
21. Park, J.-H. *et al.* Direct-Contact Microelectrical Measurement of the Electrical Resistivity of a Solid Electrolyte Interface. *Nano Lett.* **19**, 3692–3698 (2019).
22. Peled, E. & Menkin, S. Review—SEI: Past, Present and Future. *J. Electrochem. Soc.* **164**, A1703 (2017).
23. Attia, P. M., Chueh, W. C. & Harris, S. J. Revisiting the t0.5 Dependence of SEI Growth. *J. Electrochem. Soc.* **167**, 090535 (2020).
24. Han, F. *et al.* High electronic conductivity as the origin of lithium dendrite formation within solid electrolytes. *Nat Energy* **4**, 187–196 (2019).
25. Song, Y. *et al.* Probing into the origin of an electronic conductivity surge in a garnet solid-state electrolyte. *J. Mater. Chem. A* **7**, 22898–22902 (2019).
26. Vadhva, P. *et al.* Electrochemical Impedance Spectroscopy for All-Solid-State Batteries: Theory, Methods and Future Outlook. *ChemElectroChem* **8**, 1930–1947 (2021).
27. Lacey, M. Transport and transference in battery electrolytes. *Matt Lacey* http://lacey.se/science/transference/ (2023).
28. Bruce, P. G. & Vincent, C. A. Steady state current flow in solid binary electrolyte cells. *Journal of Electroanalytical Chemistry and Interfacial Electrochemistry* **225**, 1–17 (1987).
29. Evans, J., Vincent, C. A. & Bruce, P. G. Electrochemical measurement of transference numbers in polymer electrolytes. *Polymer* **28**, 2324–2328 (1987).
30. Bruce, P. G., Hardgrave, M. T. & Vincent, C. A. The determination of transference numbers in

solid polymer electrolytes using the Hittorf method. *Solid State Ionics* **53–56**, 1087–1094 (1992).

31. Balsara, N. P. & Newman, J. Relationship between Steady-State Current in Symmetric Cells and Transference Number of Electrolytes Comprising Univalent and Multivalent Ions. *J. Electrochem. Soc.* **162**, A2720 (2015).
32. Pesko, D. M. *et al.* Negative Transference Numbers in Poly(ethylene oxide)-Based Electrolytes. *J. Electrochem. Soc.* **164**, E3569 (2017).
33. Siroma, Z. *et al.* AC impedance analysis of ionic and electronic conductivities in electrode mixture layers for an all-solid-state lithium-ion battery. *Journal of Power Sources* **316**, 215–223 (2016).
34. Zarabian, M., Bartolini, M., Pereira-Almao, P. & Thangadurai, V. X-ray Photoelectron Spectroscopy and AC Impedance Spectroscopy Studies of Li-La-Zr-O Solid Electrolyte Thin Film/LiCoO2 Cathode Interface for All-Solid-State Li Batteries. *J. Electrochem. Soc.* **164**, A1133 (2017).
35. Zhao, S., Fu, Z. & Qin, Q. A solid-state electrolyte lithium phosphorus oxynitride film prepared by pulsed laser deposition. *Thin Solid Films* **415**, 108–113 (2002).
36. Osman, Z., Mohd Ghazali, M. I., Othman, L. & Md Isa, K. B. AC ionic conductivity and DC polarization method of lithium ion transport in PMMA–LiBF4 gel polymer electrolytes. *Results in Physics* **2**, 1–4 (2012).
37. Philipp, M. *et al.* The Electronic Conductivity of Single Crystalline Ga-Stabilized Cubic Li7La3Zr2O12: A Technologically Relevant Parameter for All-Solid-State Batteries. *Advanced Materials Interfaces* **7**, 2000450 (2020).
38. Lee, C., Dutta, P. K., Ramamoorthy, R. & Akbar, S. A. Mixed Ionic and Electronic Conduction

in Li3PO4 Electrolyte for a CO2 Gas Sensor. *Journal of The Electrochemical Society*.

39. Lacey, M. Electrochemical Impedance Spectroscopy. *Matt Lacey* http://lacey.se/science/eis/ (2023).
40. Electrochemical Methods: Fundamentals and Applications, 2nd Edition | Wiley. *Wiley.com* https://www.wiley.com/en-us/Electrochemical+Methods%3A+Fundamentals+and+Applications%2C+2nd+Edition-p-9780471043720.
41. Middlemiss, L. A., Rennie, A. J. R., Sayers, R. & West, A. R. Characterisation of batteries by electrochemical impedance spectroscopy. *Energy Reports* **6**, 232–241 (2020).
42. Gaberšček, M. Understanding Li-based battery materials via electrochemical impedance spectroscopy. *Nat Commun* **12**, 6513 (2021).
43. Basics of EIS: Electrochemical Research-Impedance Gamry Instruments. https://www.gamry.com/application-notes/EIS/basics-of-electrochemical-impedance-spectroscopy/.
44. Macdonald, J. R. & Barsoukov, E. *Impedance Spectroscopy: Theory, Experiment, and Applications*. (John Wiley & Sons, 2018).
45. *Lithium Batteries: Advanced Technologies and Applications*. (John Wiley & Sons, Inc., 2013). doi:10.1002/9781118615515.
46. Churikov, A. V., Gamayunova, I. M. & Shirokov, A. V. Ionic processes in solid-electrolyte passivating films on lithium. *J Solid State Electrochem* **4**, 216–224 (2000).
47. Churikov, A. V., Nimon, E. S. & Lvov, A. L. Impedance of Li□Sn, Li□Cd and Li□Sn□Cd alloys in propylene carbonate solution. *Electrochimica Acta* **42**, 179–189 (1997).

48. Lacey, M. Diffusion impedance. *Matt Lacey* http://lacey.se/science/eis/diffusion-impedance/ (2023).

49. Interfaces and Interphases in All-Solid-State Batteries with Inorganic Solid Electrolytes | Chemical Reviews. https://pubs.acs.org/doi/full/10.1021/acs.chemrev.0c00101.

50. Janek, J. & Zeier, W. G. Challenges in speeding up solid-state battery development. *Nat Energy* **8**, 230–240 (2023).

51. Doux, J.-M. *et al.* Stack Pressure Considerations for Room-Temperature All-Solid-State Lithium Metal Batteries. *Advanced Energy Materials* **10**, 1903253 (2020).

52. Yan, Z. Symmetric Cells as an Analytical Tool for Battery Research: Assembly, Operation, and Data Analysis Strategies. *J. Electrochem. Soc.* **170**, 020521 (2023).

53. Riess, I. Review of the limitation of the Hebb-Wagner polarization method for measuring partial conductivities in mixed ionic electronic conductors. *Solid State Ionics* **91**, 221–232 (1996).

54. Riess, I. Four point Hebb-Wagner polarization method for determining the electronic conductivity in mixed ionic-electronic conductors. *Solid State Ionics* **51**, 219–229 (1992).

55. Hebb, M. H. Electrical Conductivity of Silver Sulfide. *The Journal of Chemical Physics* **20**, 185–190 (2004).

56. Mizusaki, J., Fueki, K. & Mukaibo, T. An Investigation of the Hebb-Wagner's d-c Polarization Technique I. Steady-state Chemical Potential Profiles in Solid Electrolytes. *BCSJ* **48**, 428–431 (1975).

57. Huang, C.-J. *et al.* Decoupling the origins of irreversible coulombic efficiency in anode-free

lithium metal batteries. *Nat Commun* **12**, 1452 (2021).

58. Zhai, P., Liu, L., Gu, X., Wang, T. & Gong, Y. Interface Engineering for Lithium Metal Anodes in Liquid Electrolyte. *Advanced Energy Materials* **10**, 2001257 (2020).
59. Zheng, J. *et al.* Regulating electrodeposition morphology of lithium: towards commercially relevant secondary Li metal batteries. *Chemical Society Reviews* **49**, 2701–2750 (2020).
60. Li, T., Zhang, X.-Q., Shi, P. & Zhang, Q. Fluorinated Solid-Electrolyte Interphase in High-Voltage Lithium Metal Batteries. *Joule* **3**, 2647–2661 (2019).
61. Xie, J. *et al.* Fluorinating the Solid Electrolyte Interphase by Rational Molecular Design for Practical Lithium-Metal Batteries. *Angewandte Chemie International Edition* **61**, e202204776 (2022).
62. Pathak, R. *et al.* Fluorinated hybrid solid-electrolyte-interphase for dendrite-free lithium deposition. *Nat Commun* **11**, 93 (2020).